JOURNAL OF AIRCRAFT
Vol. 44, No. 2, March–April 2007

Effect of Hydrogen and Hold Time on the Lifetime of AF1410 Steel

A. Quispitupa,* B. Shafiq,† O. Uwakweh,† S. Charca,* and O. Suarez†
University of Puerto Rico, Mayagüez, Puerto Rico 00681

DOI: 10.2514/1.23516

Fatigue lifetime of model AF1410 ultrahigh-strength steel as a function of fatigue hold time (time expended at peak loads) and type and severity of environment is presented. Results indicate significant reduction in lifetime as a function of rising hold time for specimens charged with hydrogen, whereas a parabolic trend was observed in the case of specimens tested in air and in the presence of simulated marine environment. Compared with baseline tests in air, a gradual reduction in lifetime was observed as a function of increasing concentration of hydrogen in the specimens. Micrographic, atomic force microscope, and scanning electron microscope analysis is performed to study the various aspects of AF1410 lifetime.

Nomenclature

T_H = hold time (time at peak load)

I. Introduction

IT IS a common observation that various aircraft structural components undergo a loading cycle that depends on the contact time, that is, time expended at peak loads. Examples can easily be observed in arresting shanks where following a sudden rise time (time to peak loading), the near-peak load is maintained while the aircraft comes to a stop. Similar scenarios can be noticed when the landing gears come in contact with the ground, etc. Conventional laboratory fatigue testing generally ignores the short-term hold-time effects under ambient conditions as it is generally assumed that hold time (or creep-fatigue) is significant only at elevated temperatures and/or under prolonged loading times [1]. However, current investigation shows that short-term hold times under marine/ambient conditions, if not properly accounted for, can lead to serious error in lifetime estimation. A realistic testing program mimicking the actual service conditions is therefore required to properly account for the remaining lifetime.

Furthermore, for the fatigue lifetime assessment of Navy aircraft, an experimental program must address the interaction between marine environment and mechanical loading conditions, especially at the crack tip. Quantitative fatigue life predictions are very complex and in fact have never been successfully implemented, due mainly to lack of significant crack tip electrochemical/micromechanical data [2,3]. It is generally agreed that the deleterious effects of environment in high-strength steels mainly result from the effects of hydrogen that is electrochemically produced as a result of partial reaction between the metal surface and the environment [3,4]. However, quantifying the rate of production, diffusion, and egress of hydrogen into the metal surface (especially at the tip of a growing crack) is a daunting task [3], thus forcing researchers to use estimated bulk values that generally lead to inaccurate assessment of crack-tip hydrogen. Therefore, to have a quantitative and fundamental understanding of the effects of hydrogen on the fatigue crack growth, hydrogen was introduced into the alloy through laboratory-controlled electrochemical permeation process in the current study [5].

The current test program takes scarcely studied ultrahigh strength AF1410 alloy (strength $\sim$1.8 GPa and toughness $\sim$130 MPa $\cdot$ m$^{1/2}$) as a model material that has been used in the Navy's F-18E arresting shanks [6]. The objective of this investigation is to develop a fair understanding of the effects of hold time and amount of hydrogen on the fatigue life of critical aircraft components under ambient conditions. This program is significant as a large inventory of aging Navy-carrier-based aircraft fleet, while exposed to a multitude of corrosive agents, operates under extremely high flight loads with frequent landings and takeoffs [3,7]. The expected outcome is the reasonably good data that can be used to better estimate the remaining lifetime of aircraft components.

II. Experimental Setup

Critical aircraft components, such as arresting shanks or landing gears, undergo a sudden rise time followed by a hold time at peak load. Therefore, to properly simulate such fatigue scenario, a high rise/descent rate of loading of 100,000 N/s was established, dictated mainly by the equipment limitations, whereas the hold time was varied from 0 to 60 s. Hold-time testing was conducted under load control trapezoidal waveform. The waveform corresponding to hold-time testing is depicted in Fig. 1a. At each hold time, testing was performed on 1) specimens in air, 2) specimens in the presence of mild 3.5%NaCl of pH $\sim$ 2.5 (simulating crack-tip pH) electrolyte, and 3) on specimens symmetrically charged with hydrogen for 82 h, inducing hydrogen on the average to over 95% penetration depth into the specimen [2,4,8,9].

Furthermore, to obtain a quantitative understanding of the effects of hydrogen on AF1410 steel, fatigue testing was performed on specimens charged with hydrogen at various concentration levels. Hydrogen charging was performed by subjecting the two surfaces to cathodic polarization simultaneously [5]. One surface was galvaonstatically charged, whereas the other surface was potentistated. This ensured that approximately equal amounts of hydrogen were introduced on both surfaces. Micrographical and scanning electron microscope (SEM) evidence indicates that this arrangement introduced a fairly uniform distribution of hydrogen in the steel. Specimens were charged in a controlled manner from 0 to (a limiting case of) 84 h, permeating hydrogen to an estimated depth of 0 mm to over 95% penetration on both sides of the specimen. The micrograph in Fig. 2 illustrates the typical hydrogen penetration depths as a function of charging time. The hydrogen concentration scenarios are relevant as hydrogen flux is generally not possible in realistic aircraft components, and as a result, significant hydrogen remains only in the vicinity of the metal surface where it manifests localized embrittlement, leading to subsequent crack initiation and

Received 27 February 2006; revision received 28 November 2006; accepted for publication 5 December 2006.

*Graduate Student, School of Engineering, Department of Civil Engineering, Box 9041.
†Associate Professor, School of Engineering, Department of General Engineering, Box 9044.

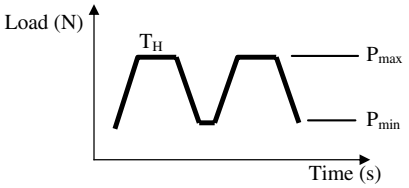

a) Hold time

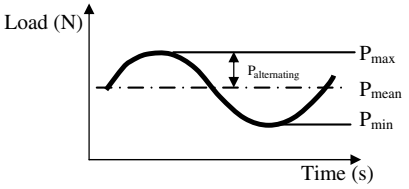

b) Load decrementing

Fig. 1 Loading waveform for fatigue testing.

growth under stress. This part of testing was performed in strain control under a sinusoidal waveform (as sketched in Fig. 1b) at a frequency of 0.5 Hz, and at values corresponding to 50% of the quasi-statically obtained yield strain [2].

All testing was conducted at room temperature on compact-tension (CT) specimens of dimensions $5 \times 4 \times 0.32$ cm at R(loading ratio) $= 0.3$. Furthermore, all specimens were precracked according to the ASTM E399-95 standard. Quasi-static tests performed at various rates of loading between 8 and 15,000 N/s yielded virtually the same ultimate static strength of about 38 kN, indicating that AF1410 was not sensitive to static rate of loading under ambient conditions. Crack length was measured using a compliance technique that has been proven reliable in crack growth studies of AF1410 steel [2,10]. Periodic visual inspection was also performed to verify compliance-based crack lengths. SEM that has been widely used in the study of microcrack nucleation and growth, striation shapes, slip bands, and to extract general failure features of a variety of materials was used for fracture surface analysis to corroborate and further understand failure mechanisms and shifts in the modes of failure [4].

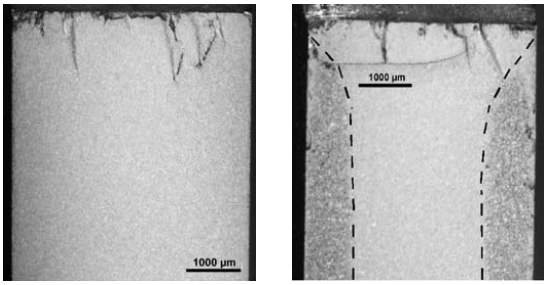

a) Charging time = 0h **b) Charging time = 3h**

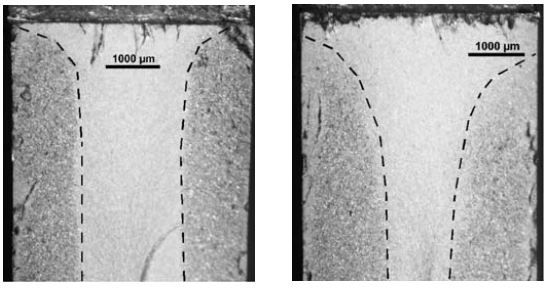

c) Charging time = 11h **d) Charging time = 21h**

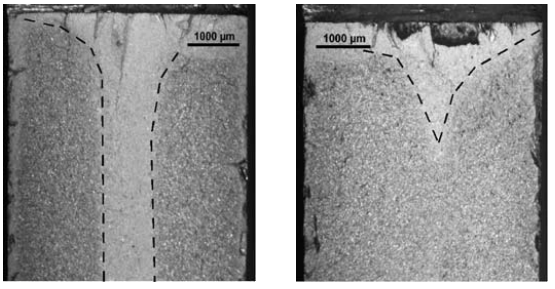

e) Charging time = 42h **f) Charging time = 84h**

Fig. 2 Micrographs showing typical hydrogen penetration depths as a function of charging time.

III. Experimental Results

An almost complete loss of life was observed as the hold time increased from 0 to 10 s in the hydrogen-charged specimens, as shown in Fig. 3a. In contrast, lifetime behavior consistently depicted an increase in lifetime as a function of increasing hold time (roughly from 0 to 5 s) followed by a gradual decrease for specimens tested in air or in the presence of 3.5% NaCl, also seen in Fig. 3a. Figure 3b shows a summary of typical lifetime data for specimens tested under various conditions corroborating the results of Fig. 3a, that is, a sharp decrease in lifetime for hydrogen-charged specimens and a parabolic trend for the specimens tested in air and in the presence of electrolyte. Figures 4a and 4b show comparison of crack growth rates (CGRs) at typical hold times for specimens tested in air, in the presence of 3.5% NaCl, and charged with hydrogen. Almost an order of magnitude difference in the CGR is observed between hydrogen-charged specimens and the ones tested in air and 3.5% NaCl. Interestingly, Figs. 4a and 4b show no discernible change in the CGR between specimens tested in air and in the presence of 3.5% NaCl electrolyte; however, this is mainly due to the nature of logarithmic presentation, which serves to diminish small variations in the data.

Figures 5a and 5b illustrate the dramatic but gradual reduction in the number of cycles to failure as a function of increasing charging

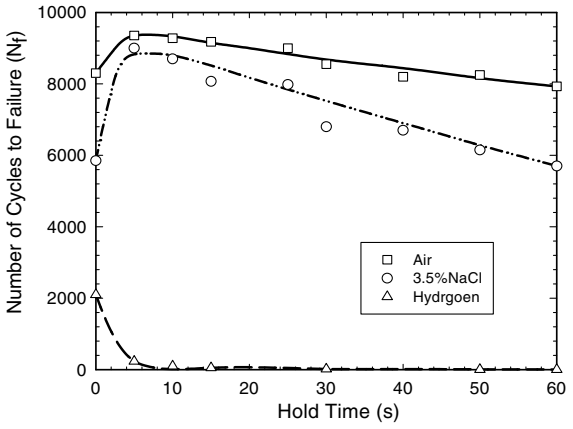

a) Number of cycles to failure as a function of hold time T_H

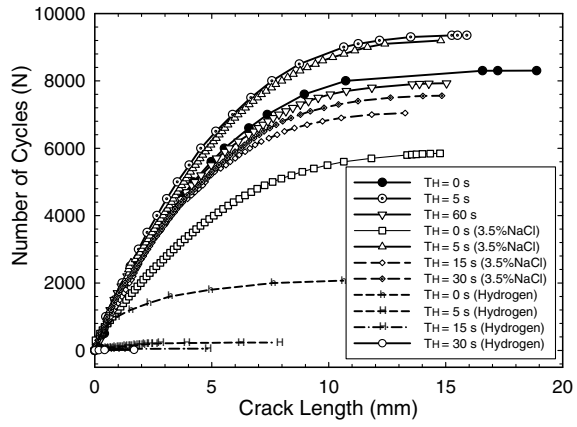

b) Crack length vs number of cycles at typical hold times

Fig. 3 Fatigue lifetime for specimens tested in air, in the presence of 3.5% NaCl electrolyte, and electrochemically charged with hydrogen.

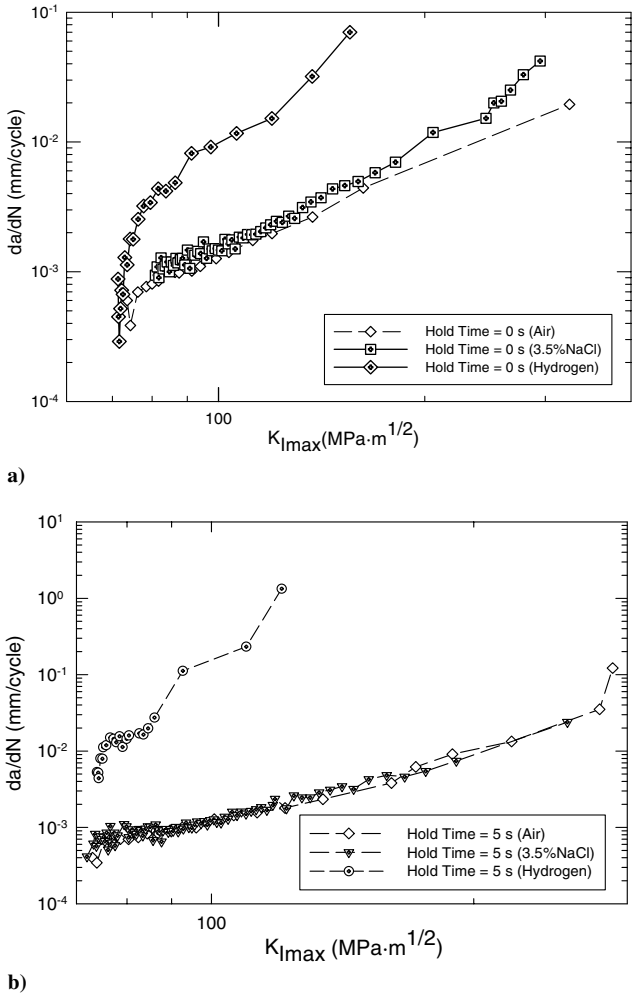

Fig. 4 Typical CGR as a function of hold time.

time (hydrogen permeation depth), whereas Fig. 5c shows the typical CGR results at various charging times. It should be noticed that Fig. 4 results are based on the load control testing whereas Fig. 5 depicts strain control test results [2].

IV. Results and Discussion

An expected behavior was observed in the case of hydrogen-charged tests, namely, increasing the charging time led to reduction in lifetime (Fig. 5), which agreed well with the reported literature [11]. On the other hand, hold-time test results unveiled several interesting features of the alloy tested. It is generally expected that hold time at ambient conditions would have little to no effect on the lifetime of the high-strength alloys and that such alloys are only significantly affected either under prolonged creep loading or at higher temperatures [1]. However, the CGR results observed in Figs. 3a and 3b indicate a sharp decreasing trend in the case of hydrogen-charged samples and a parabolic trend in the case of samples tested in air or in the presence of 3.5% NaCl. The loss of life due to the presence of NaCl electrolyte under various hold times can also be observed in Fig. 3, though significantly less pronounced compared to hydrogen-charged specimens. The contrast in lifetime behavior between hydrogen-charged specimens and those subjected to NaCl electrolyte points in general terms to loss of coherency and brittle behavior in the first case and competing mechanisms of coherency and strain hardening followed by dislocation mobility and ion migration in the latter. However, to understand the results (of hydrogen charging and hold time), it is necessary to obtain a clear understanding of the competing crack advance (impedance) mechanisms, namely, the mechanical effects resulting from heightened stress intensity, dislocation-induced microstructural changes, and crack-tip electrochemical processes.

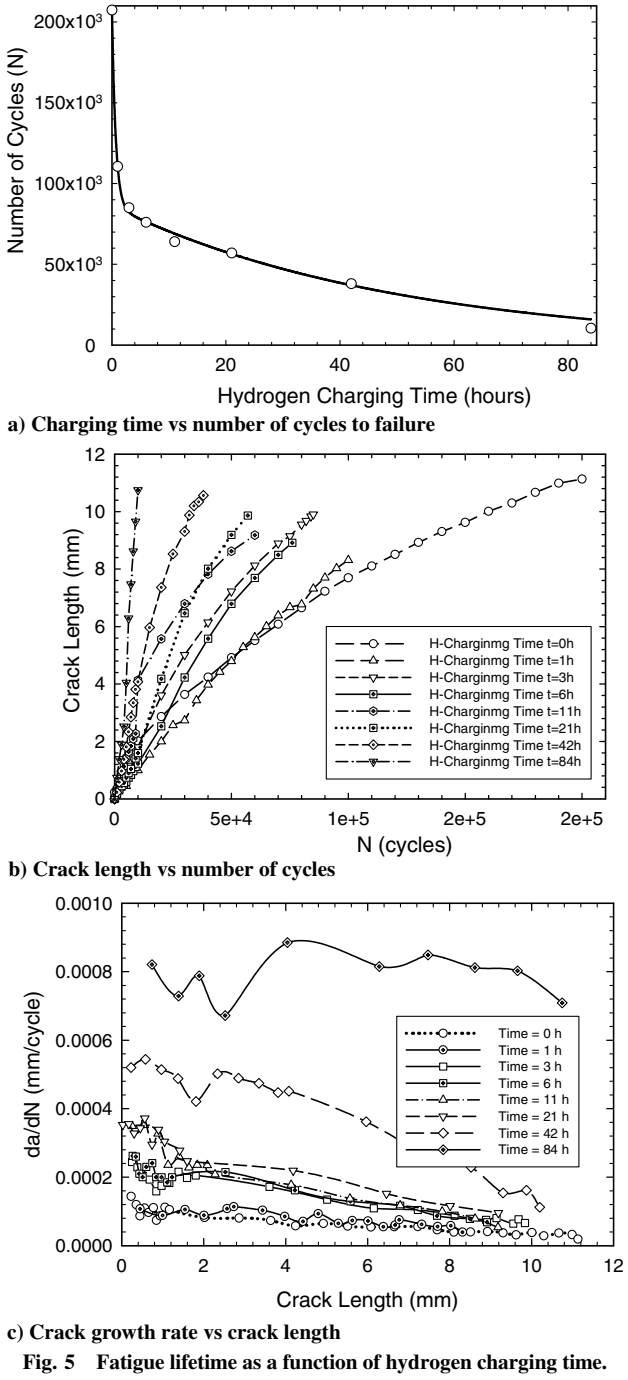

Fig. 5 Fatigue lifetime as a function of hydrogen charging time.

To account for the effect of hydrogen concentration and the parabolic trend observed in laboratory-air-tested and NaCl-induced AF1410 steel specimens (Fig. 3), one must consider the effects of microstructure on the toughening mechanisms of multiphased materials. AF1410 steel is ultrahigh-strength steel derived from its multiphased nature, which depends on applied heat treatments. The phases present in AF1410 steel include lath martensite, some retained austenite, bainite, and carbide, as shown in Fig. 6. After age hardening at 950 $\pm$ 10°F, the material consists of a highly dislocated lath martensite, with a small amount of stringerlike retained austenite at the interlath boundaries [6]. Furthermore the precipitates are shown being very fine, and are located in the interior of the lath and between the lath. These particles are small sized, and so it has been concluded that the precipitation agent at the indicated temperature of treatment produced a fine $(MoCr)_2C$ [6,12]. These (small size) finely dispersed particles seem to nucleate at dislocations. Additionally, the carbide phases are generally finely dispersed, and of the coherent type, though cementite, $(MoCr)_2C$ could be observed following

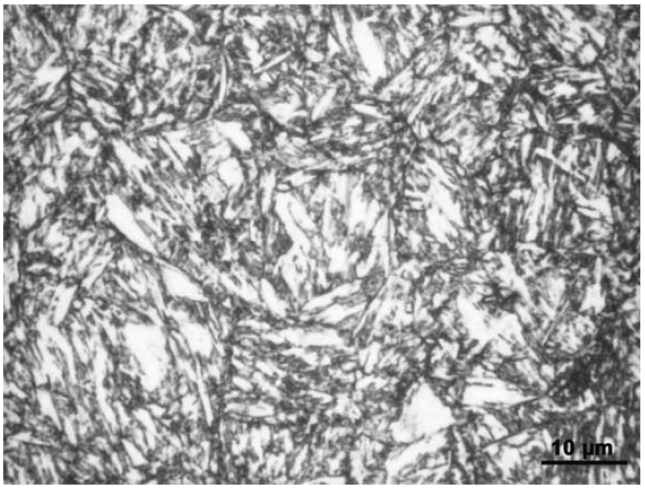

Fig. 6 Micrograph showing the microstructure of AF1410 steel.

high-temperature aging/tempering. Complex carbides, which generally are of the coherent types, are usually based on the $(MoCr)_2C$ and may even include $(MoCrFe)_2C$ types as well. The transient Fe-based carbides such as the η-carbides are precursors to the ε-carbides that form at fairly lower temperatures before the formation of the cementite, or Fe_3C at higher temperatures with or without χ-carbides.

The best microstructures for combining toughness with strength are strengthened with fine particles, which are finely dispersed and well bonded to the matrix. In other words, if the interface between the particles and the matrix are the coherent types, then microvoid formation by decohesion will be avoided or made difficult. For this to be the case, it is expected that the particles be no more than 100 μm to minimize chances of multiple slip-band pileups, which would greatly enhance local pileup stress, and create decohesion or particle fracture from occurring. Dispersion is expected to avoid overlap of stress fields, whereas rounded or spherical forms would help eliminate stress concentration associated with corners, and should be equi-axed as possible to avoid the multiple pileup effects.

A. Effect of Hydrogen

With hydrogen charging, hydrogen is expected to migrate to the high-strain fields (such as crack tip) associated with coherent and semicoherent interfaces of the finely dispersed complex carbide precipitates. During strain application following fatigue test, the hydrogen-carbide atmosphere would change because a breakup of the interfaces will occur, which would translate to decrease or loss in strength. Therefore, an increased amount of hydrogen would make crack-tip failure (and enhanced CGR) more likely as a result of increasing loss of coherency [3,13].

In the case of semicoherent interfaces between the carbides and matrix, it is expected that hydrogen would preferentially lodge around the dislocations in the martensite and banite phase. During stress application, loss of strength can only result if hydrogen enhances particle cutting (incoherency). Because the chance of this is remote, therefore, hydrogen atmosphere around semicoherent or incoherent surfaces would not explain the continuous drop in or loss of strength observed in the tests.

The ideas of reversible and irreversible trapped hydrogen play an important role in understanding the effects of hydrogen on the lifetime of alloys. For example, during the fatigue loading, the *reversible trapped hydrogen* (RTH) (limited resident time) can move through dislocations (highly dislocated lath martensite) to localize into microstructural sites, such as faults, vacancies, and grain boundaries, or to produce new dislocations [14]. As a result the hydrogen concentration at these places can be enhanced. The hypothesis is that upon stressing, H-repartitions from low to moderate strength RTH sites and is attracted to the crack tip stress field. In addition, RTH movement induces a recombination of H-

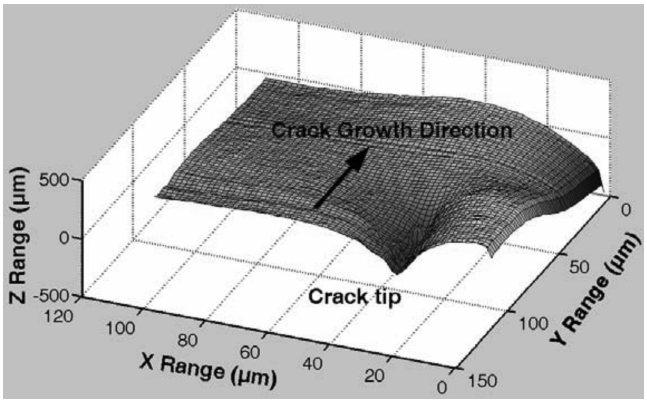

Fig. 7 AFM image showing plasticity at the tip of the growing crack.

atoms at internal microvoids or microcracks that can lead to high atomic hydrogen pressure sufficient to enlarge and grow these microfaults, thus aiding in the progressive failure of the alloy. Therefore, an increase in the H-concentration increases the level and mobility of RTH and subsequently to an increase in the crack tip embrittlement and CGR as seen in Fig. 5. RTH mobility, which is linked to the lifetime reduction, is also expected to rise in hydrogen-charged specimens at longer hold times, especially under higher stress intensity factors (i.e., at stage 2 under load control test conditions). On the other hand, the *irreversible trapped hydrogen* (ITH) has permanent resident time into the material under ambient conditions accompanied by high activation energy, and as a result its mobility is limited [14]. Therefore, it is believed that ITH does not contribute significantly in the embrittlement process and hence would not be a contributing factor in the observed fatigue lifetime reduction.

Another important mechanism that must be taken into account where hydrogen is present is the *hydrogen-enhanced local plasticity* [3,4,13]. The atomic force microscope (AFM) image in Fig. 7

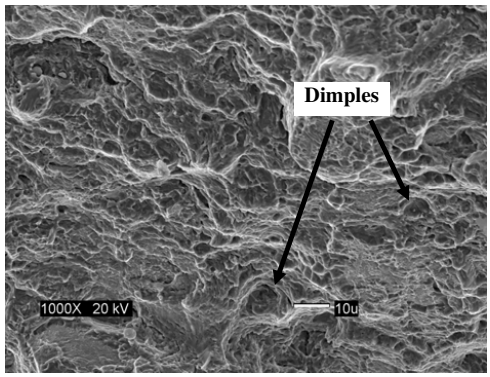

a) Hold time = 0 s

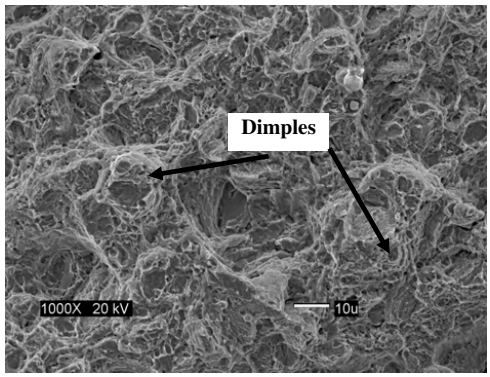

b) Hold time = 5 s

Fig. 8 Fracture surface morphology showing the dimpled surface for a hydrogen-charged specimen at 0 and 5 s hold time.

illustrates the crack-tip plastic deformation, a process that is exacerbated as the hydrogen concentration increases. This phenomenon was observed in the fracture surface analysis as a macroscopically reduced ductility around the crack tip and a brittle appearance of the fractured surface at low magnifications. The enhanced local plasticity can be seen in the form of a dimpled fracture surface as depicted in the SEM images of Fig. 8 [4]. The sizes of dimples or microvoids are affected by the presence of the second phase particles ($(MoCr)_2C$, $(MoFe)_xC$, $(Fe, Ni, Co)_3C$), etc. [15]) of coherent, semicoherent, and incoherent nature. It is speculated that dimple size is a function of hold time and hydrogen concentration as the localized plasticity implies that strain hardening coefficient of the material would change and that would lead to the variations in dimple size. The hydrogen permeated into the steel tends to accumulate at the interface of the second phase particles; however, the coherent and semicoherent locations are preferable for RTH and the incoherent for ITH [14]. As a result, RTH appears to affect the nucleations of microvoids at the particle–matrix interface, thus increasing the microvoid density and decreasing the average size.

Some low-resolution SEM images shown in Fig. 9 clearly indicate a shift in the modes of failure for specimens partially charged with hydrogen. On the portion charged with hydrogen (Fig. 9a), predominantly intergranular (IG) brittle features with transgranular (TG) pockets can clearly be observed, indicating the embrittlement effects of hydrogen. Whereas at the interface representing the extent of hydrogen penetration depth (Fig. 9b), a mixed ductile (on the upper side) and brittle (on the lower side) mode of failure is noticed. On the portion of the specimen devoid of hydrogen (Fig. 9c), mainly microvoid (MV) ductile features are observed.

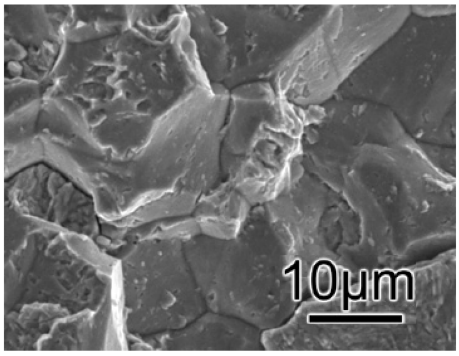

a) IG brittle features in the hydrogen-charged portion of the specimens

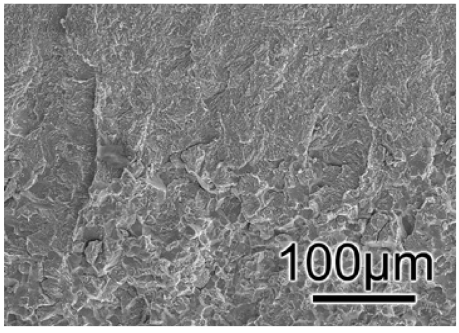

b) Mixed mode ductile-brittle failure at the interface

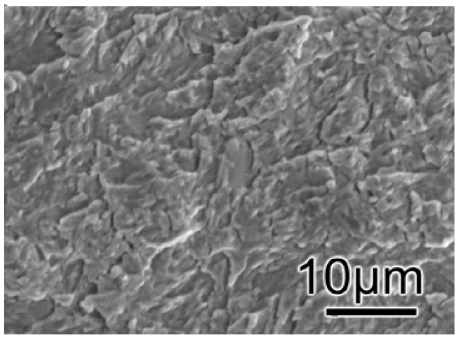

c) Mainly MV ductile features on the portion devoid of hydrogen

Fig. 9 SEM images of fracture surface morphology.

B. Lifetime of Uncharged Samples

Martensitic phase is generally more stable, and as a result, austenitic transformation into martensite can lead to strengthening (as may be the case in the uncharged samples) or presence of hydrogen in austenite can prevent this martensitic transformation (as in the case of charged samples). Therefore, in the uncharged samples, initial increase in strength can be explained from the combination of factors, such as toughening due to austenitic to martensitic transformation that is strain induced. The absence of this in the hydrogen-charged samples can be explained from the elimination of this transformation due to prior hydrogen-induced transformation of some of the retained austenite, or the stabilization of the austenitic phase due to solid solution solute interaction with hydrogen. Thus, both laboratory-air- and NaCl-induced samples would not be affected to the same degree as with hydrogen-charged ones. Though Cl^- ions are known to provoke loss of strength due to corrosion, the effect is not as far reaching as hydrogen introduced via cathodic polarization [6,16].

When NaCl is present in the aqueous solution, Cl^- exacerbates the anodic/cathodic reaction and preferentially migrates to the crack tip through combined diffusion and electrolysis. This process weakens materials atomic bonds and enhances local stress intensity, which contributes in the observed lifetime reduction, as compared to air tested samples (Fig. 3) [2]. Additionally, combination of stress and presence of NaCl electrolyte in H_2O causes the H^+ and OH^- ions to be "freed" more than otherwise and causes the dissociation of Na^+ and Cl^- ions such that overall conduction activity is increased. Simultaneously with Cl^- activity, H^+ gets dissolved as well in the material, thereby weakening the material through reduction in bond strength. H^+ is much smaller than Cl^- and therefore diffuses faster than Cl^-. The H^+ and OH^- produced subsequently capture and move with the vacancies, thus enhancing dislocation mobility [3,4,17].

Immobile dislocations cause an increase in strength, and conversely, dislocation mobility increases as a function of the fatigue loading. Therefore, in the uncharged samples, coherency can cause an increase in CGR up to a point (threshold), beyond which dislocation mobility, effect of H^+ and OH^-, and Cl^- migration would lead to loss of strength, as observed in Figs. 2a and 2b

V. Conclusions

Lifetime performance of AF1410 is found to be highly dependent upon the level of hydrogen concentration. Hold-time tests indicated a sharp decreasing trend as the hold time is increased in the case of hydrogen charges samples and a parabolic trend in the case of lab-air- and NaCl-environment-tested samples. The results are discussed from the microstructural considerations and corroborated with micrographic, SEM, and AFM analysis.

Acknowledgments

The research was carried out under Office of Naval Research (ONR) grant no. N000140310540. The authors wish to acknowledge the ONR program manager Yapa Rajapakse for his support and guidance. Thanks are also due to Vinod Agarwala, senior scientist at Naval Air Warfare Center–Aircraft Division, for his encouragement to undertake this task.

References

[1] Nicholas, T., and Weerasooriya, T., "Hold-Time Effects in Elevated Temperatures Fatigue Crack Propagation," *Fracture Mechanics*,

Vol. 17, ASTM STP 905, American Society for Testing and Materials, Philadelphia, 1986, pp. 155–168.

[2] Quispitupa, A., Shafiq, B., Suárez, O. M., Uwakweh, O. N. C., Duque, N., "Corrosion Fatigue of High-Strength Aircraft Structural Alloys," *Journal of Aircraft* (to be published).

[3] Turnbull, A., "Modeling of Environment Assisted Cracking," *Corrosion Science*, Vol. 34, No. 6, 1993, pp. 921–960.

[4] Beachem, C., "A New Model for Hydrogen-Assisted Cracking (Hydrogen Embrittlement)," *Metallurgical Transactions*, Vol. 3, 1972, pp. 437–451.

[5] Charca, S., Uwakweh, O. N. C., Agarwala, V. A., "Hydrogen Transport in Cathodically Polarized AF1410 Steel: Hydrogen Transport Conditions and Effects," *NACE: Tri-Service Corrosion Conference, Session on Corrosion Mechanisms and Kinetics*, Orlando, FL, Nov. 2005.

[6] Antolovich, S., "Fatigue Crack Propagation and Corrosion Fatigue of AF1410 Steel," Air Force Materials Laboratory-Air Force System Command, Technical Report AFML-TR-79-4209, Wright–Patterson Air Force Base, OH, May 1978.

[7] Agarwala, V., "What's Eating Us: Corrosion," *Naval Research Reviews*, Vol. 50, No. 4, 1998, pp. 14–24.

[8] En-Hou, H., and Wei, K., "Chemical and Electrochemical Conditions within Corrosion Fatigue Cracks," *Corrosion Science*, Vol. 35, Nos. 1–4, 1973, pp. 599–610.

[9] Boodey, J., and Agarwala, V., "Hydrogen in Metals: Cadmium Plated Steel," Paper 224, *Corrosion87*, San Francisco, CA, 1987, pp. 224/1–224/11.

[10] Saxena, A., and Hudak, S., "Review and Extension of Compliance Information for Common Crack Growth Specimens," *International Journal of Fracture*, Vol. 14, No. 5, 1978, pp. 453–468.

[11] Thomas, R. L. S., Scully, J. R., Gangloff, R. P., "Internal Hydrogen Embrittlement of Ultrahigh-Strength AERMET 100 Steel," *Metallurgical and Materials Transactions A: Physical Metallurgy and Materials Science*, Vol. 34A, No. 2, 2003, pp. 327–344.

[12] Ayer, R., Machmeier, P. M., "Microstructural Basis for the Effect of Chromium on the Strength and Toughness of AF1410-Based High Performance Steel," *Metallurgical and Materials Transactions A: Physical Metallurgy and Materials Science*, Vol. 27A, 1996, pp. 2510–2517.

[13] Birnbaum, H. K., "Mechanisms of Hydrogen Related Fracture of Metals," *Proceedings of Fourth International Conference on the Effects of Hydrogen on the Materials Behavior*, edited by Neville R. Moody and Anthony E. Thompson, TMS Publications, Warrendale, PA, 1989, pp. 639–660.

[14] Li, D., Gangloff, R. P., Scully, J. R., "Hydrogen Trap States in Ultrahigh-Strength AERMET 100 Steel," *Metallurgical and Materials Transactions A: Physical Metallurgy and Materials Science*, Vol. 35A, 2004, pp. 849–864.

[15] Jemian, P. R. L., "Characterization of Steels by Anomalous Small-Angle X-Ray Scattering," Ph.D. Dissertation, Northwestern Univ., Evanston, IL, June 1990, pp. 5–8.

[16] DeLucia, J. J., "Electrochemical Aspects of Hydrogen in Metals," *Hydrogen Embrittlement: Prevention and Control*, STM STP 962, edited by L. Raymond, American Society for Testing and Materials, Philadelphia, 1988, pp. 17–34.

[17] Tien, J., Thompson, A., Bernstein, I., Richards, R., "Hydrogen Transport by Dislocations," *Metallurgical Transactions A (Physical Metallurgy and Materials Science)*, Vol. 7A, 1976, pp. 821–829.